25th ABCM International Congress of Mechanical Engineering
October 20-25, 2019, Uberlândia, MG, Brazil

COB-2019-1016
FLOWS OF ELASTO-VISCOPLASTIC MATERIALS APPROXIMATED BY A STABILIZED FINITE ELEMENT METHOD

Vitor Dal Bó Abella
Natan Alexandre de Oliveira
Sérgio Frey
Departament of Mechanical Engineering, Federal University of Rio Grande do Sul - Rua Sarmento Leite, 425 – 90050-170 – Porto Alegre, RS, Brazil
vitor.abella@mecanica.ufrgs.br, natan.oliveira@mecanica.ufrgs.br, frey@mecanica.ufrgs.br

Abstract. *The present work studies the flow of an elasto-viscoplastic fluid through a sudden four-to-one contraction. Mechanical modeling makes use of an Oldroyd-B viscoelastic equation modified to allow that either the elastic times or the polymeric viscosity are rheology-dependent. A three-field Galerkin least-squares method is used in terms of extra-stress, velocity, and pressure, to approximate the model. Results focus on the influence of the flow intensity on the yield surfaces, elasticity and relaxation time. Clear interlace is verified between these parameters and the position and shape of yield surfaces.*

Keywords: *elasto-viscoplasticity, viscoplastic materials, sudden contraction, stabilized method*

1. INTRODUCTION

The study of non-Newtonian fluids is of scientific and industrial relevance since their significant presence in industrial applications. To list only a few, there are polymeric extruder flows in the plastic industry, manufacture of gels and shampoos and inks in the cosmetic industry and perforation muds in oil industry (Mahmood *et al.*, 2017).

According to Bingham (1922), when the viscoplastic behavior is present in the fluid, the yield stress must be achieved to the fluid start to flow. If the internal stress is lower than the yield stress, the material doesn't flow. Those regions on which yield stress is not surpassed are called unyielded regions, and the interface between unyielded and yielded regions are known as yield surfaces. Barnes (1999a,b) claimed that the *yield stress* doesn't exist, contradicting the classical definition. There is a huge increase (but finite) in the viscosity near the yield stress. This new definition created the so-called apparent yield stress fluids. Besides, studies verified elastic behavior within unyielded regions – see, for instance, (Gueslin *et al.*, 2006; Putz *et al.*, 2008; Sikorski *et al.*, 2009), and reference therein. Also, elasto-viscoplastic materials may present thixotropic behavior as investigated by (Balmforth *et al.*, 2014; Coussot, 2014).

Complex flows are frequent in industrial processes and in Nature. Accidents imposed by complex geometries induce to geometric nonlinearities, such as back-flow recirculations and flow detachments. In the particular of Non-Newtonian flows, their material equations add material nonlinearity to the mechanical modeling employed. Complex fluids as elasto-viscoelastic and thixotropic ones, induce to striking effects when flowing through complex geometries – such as memory and non-zero normal stress differences.

In the last decade, some authors have investigated numerically and proposed constitutive equations for this class of material. Nassar *et al.* (2011) simulated elasto-viscoplastic materials in axisymmetric expansion-contraction flows using a model based on the one proposed by de Souza Mendes and Dutra (2004). Belblidia *et al.* (2011) approximated an axisymmetric expansion-contraction flow through a 4:1:4 contraction-expansion channel, with the BWW model introduced by the authors. Santos *et al.* (2014) studied the elasto-viscoplastic flows numerically through a duct subjected to an expansion-contraction using the model proposed by de Souza Mendes (2011). Link *et al.* (2015) computed a thixotropic flow over a 1:4 sudden expansion using the model intropuced by de Souza Mendes (2011). Fraggedakis *et al.* (2016) compared five recent proposed elasto-viscoplastic models proposed by Saramito (2007, 2009); Park and Liu (2010); Belblidia *et al.* (2011) in the flow around around a falling spherical particle. López-Aguilar *et al.* (2016) contrasted the models proposed by López-Aguilar *et al.* (2014) and de Souza Mendes (2011) in thixotropic flow over an axisymmetric contraction-expansion. Oishi *et al.* (2017) evaluated the avalanche-effect of an thixopic elasto-vicoplastic flows over an inclined plane using de Souza Mendes and Thompson (2013) model.

The current article uses the thixotropic equation proposed by de Souza Mendes (2011) to predict elastic, viscoplastic and shear-thinning effects in a yield stress material that flows through a four to one sudden contraction. The model is approximated by a three-field Galerkin least-squares–like method, in terms of extra stress, pressure, and velocity, aiming

at allowing the use of Lagrangean finite elements, and to improve the convergence of Galerkin method.

2. MATHEMATICAL FORMULATION

2.1 Elasto-visco plastic model

The constitutive model used here is based on a Oldroyd-B formulation of an elasto-visco plastic thixotropic model introduced by de Souza Mendes (2011). In this formulation the viscosity and the elastic modulus are function of the structure parameter. The stress was split using the e elastic-viscous-split-stress (EVSS) scheme (Rajagopalan *et al.*, 1990), where the extra stress is decomposed in its viscous and elastic contribution.

$$\boldsymbol{\tau} = \boldsymbol{\tau}_1 + \boldsymbol{\tau}_2 \tag{1}$$

$$\boldsymbol{\tau}_2 + \theta \overset{\nabla}{\boldsymbol{\tau}}_2 = 2\eta_s \left(\mathbf{D}(\mathbf{u})\right) \tag{2}$$

$$\boldsymbol{\tau}_1 = 2\eta_\infty \boldsymbol{D}(\boldsymbol{u}) \tag{3}$$

Where η_s is the structural viscosity and $\overset{\nabla}{\boldsymbol{\tau}}$ denotes the upper-convected derivative of the extra stress:

$$\overset{\nabla}{\boldsymbol{\tau}} = (\nabla \boldsymbol{\tau})\mathbf{u} - (\nabla \mathbf{u})\boldsymbol{\tau} - \boldsymbol{\tau}(\nabla \mathbf{u})^T \tag{4}$$

The relaxation time, θ, from Eq. (2) is defined as:

$$\theta(\lambda) = \left(1 - \frac{\eta_\infty}{\eta_s(\lambda)}\right) \frac{\eta_s(\lambda)}{G(\lambda)} \tag{5}$$

As η_∞ corresponds to the low viscosity region, Equation (5) simplifies to:

$$\theta(\lambda) = \frac{\eta_s(\lambda)}{G(\lambda)} \tag{6}$$

Following (de Souza Mendes, 2011), the dependence of elastic modulus, G, on structure parameter λ is given by:

$$G(\lambda) = G_0 \exp\left(m\left(\frac{1}{\lambda} - 1\right)\right) \tag{7}$$

In the Eq. (7), G_0 is the structural elastic modulus of a fully structured material, and m is a positive scalar parameter that dictates the sensitivity of G with λ.

This model consider the microestructure of the material. The structure parameter λ is thus a scalar-valued distribution that ranges from 0 to 1 and maps the structuring level of the microstructure. For $\lambda = 1$ the material is fully-structured, the model predicts elastic body behavior and, for $\lambda = 0$ the material is fully unstructured with the model predicting a pure viscous behavior. For $0 < \lambda < 1$, the model predicts a viscoelastic behavior. It is clear that this formulation assumes that there is a one-to-one relationship between the structuring level and viscosity levels:

$$\eta_s(\lambda) = \left(\frac{\eta_0}{\eta_\infty}\right)^\lambda \eta_\infty \tag{8}$$

The Eq. (8) can be solved to λ:

$$\lambda(\dot{\gamma}) = \frac{\ln \eta_s(\dot{\gamma}) - \ln \eta_\infty}{\ln \eta_0 - \ln \eta_\infty} \tag{9}$$

where η_0 and η_∞ are the zero and infinite-shear-rate viscosities, respectively, $\dot{\gamma} \equiv (\frac{1}{2} \operatorname{tr} \mathbf{D}(\mathbf{u})^2)^{1/2}$ is the magnitude of strain rate tensor $\mathbf{D}(\mathbf{u})$ and η_s is the structural viscosity.

The evolution of λ is given by:

$$\frac{D\lambda}{Dt} = \frac{1}{t_{eq}} \left[(1 - \lambda) - f(\tau)\lambda\right] \tag{10}$$

Where $f(\tau)$ is a function that is zero at $\tau = 0$ and increases monotonically as τ is increased. The thixotropic equilibrium time, t_{eq}, characterizes the time of change of λ.

The model herein assumed that once its microstructure is broken due to a stress change, the material reestablishes its thermodynamical equilibrium instantaneously. In this condition, the thixotropic equilibrium time t_{eq} tends to zero and the structure parameter is always in equilibrium. The equilibrium structure parameter λ_{eq} can thus be seen as a normalized equilibrium viscosity function.

As the fluid is always in structural equilibrium, $\eta_s = \eta_{eq}$, $G = G_{eq}$ and $\theta = \theta_{eq}$ where the subindex eq denotes the equilibrium sctructure value of the variable.

In this work, the following expression for the equilibrium viscosity was employed, from de Souza Mendes (2007):

$$\eta_{eq}(\dot{\gamma}) = \left[1 - \exp\left(-\frac{\eta_0 \dot{\gamma}}{\tau_y}\right)\right]\left\{\frac{\tau_y}{\dot{\gamma}} + K\dot{\gamma}^{n-1}\right\} + \eta_\infty \tag{11}$$

Where τ_y is the yield stress, K the consistency index and n the power-law index.

2.2 Balance equations and problem statement

The fluid is assumed to be incompressible, gravitational force is neglectable and the flow is considered inertialess. For this case, consider an open domain $\Omega \subset \Re^2$, the balance of mass and momentum are:

$$\operatorname{div} \boldsymbol{u} = 0 \quad \text{in } \Omega \tag{12}$$

$$\mathbf{0} = -\nabla p + \operatorname{div} \boldsymbol{\tau}_2 + 2\eta_\infty \operatorname{div}(\boldsymbol{D}(\boldsymbol{u})) \quad \text{in } \Omega \tag{13}$$

Where $\boldsymbol{u}$ is the velocity vector, p is the pressure and $\boldsymbol{\tau}$ is defined in Eq. (2), The geometry domain is an axial symmetric planar contraction 4:1 and the no-slip hypothesis is considered at the wall. The inlet is a developed profile in terms of pressure, velocity and stress. The problem statement is represented in Fig. 1.

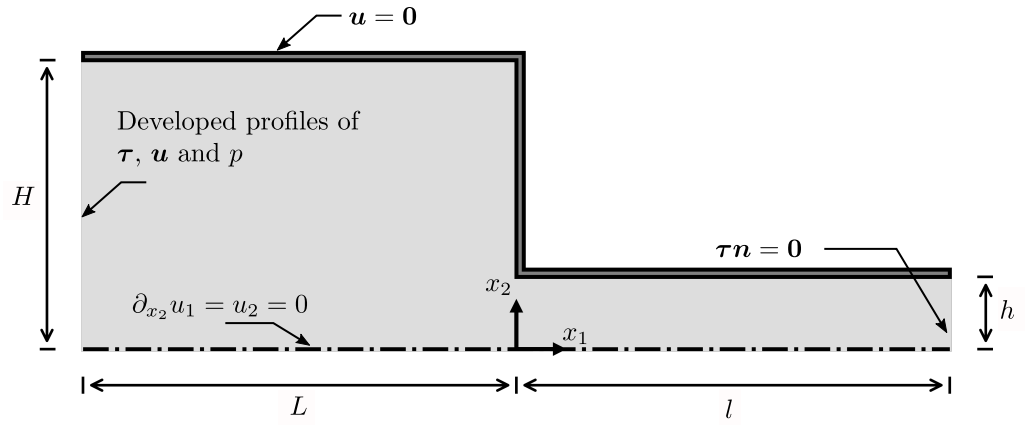

Figure 1: The problem statement.

The numerical scheme employed to solve the problem is finite element multifield Galerkin least-squares in terms of velocity, pressure and extra stress proposed by Franca and Frey (1992).

2.3 Dimensionless equations

As discussed in de Souza Mendes (2011), three shear rates mark important transitions in the flow curve, namely $\dot{\gamma}_0, \dot{\gamma}_1$, and $\dot{\gamma}_2$. The $\dot{\gamma}_0$ is the maximum shear rate in which the material remains at η_0. $\dot{\gamma}_1$ marks the beginning of the power-law region. Above $\dot{\gamma}_2$ the material structure is destroyed, representing the transition between power law to Newtonian.

$$\dot{\gamma}_0 = \frac{\tau_y}{\eta_0}\,, \quad \dot{\gamma}_1 = \left(\frac{\tau_y}{K}\right)^{1/n}, \quad \dot{\gamma}_2 = \left(\frac{\eta_\infty}{K}\right)^{1/n-1} \tag{14}$$

The equations are adimensionalized as proposed by de Souza Mendes (2007):

$$\begin{gathered} G_0^* = \frac{G_0}{\tau_y} \quad G_{eq}^* = \frac{G_{eq}}{\tau_y} \quad p^* = \frac{p}{\tau_y} \quad \eta_0^* = \frac{\eta_0 \dot{\gamma}_1}{\tau_y} \quad \eta_\infty^* = \frac{\eta_\infty \dot{\gamma}_1}{\tau_y} \quad \eta_{eq}^* = \frac{\eta_{eq} \dot{\gamma}_1}{\tau_y} \quad \theta_{eq}^* = \dot{\gamma}_1 \theta_{eq} \\ \boldsymbol{\tau}^* = \frac{\boldsymbol{\tau}}{\tau_y} \quad \dot{\boldsymbol{\gamma}}^* = \frac{\dot{\boldsymbol{\gamma}}}{\dot{\gamma}_1} \quad \boldsymbol{u}^* = \frac{\boldsymbol{u}}{\dot{\gamma}_1 h} \quad \boldsymbol{x}_1^* = \frac{\boldsymbol{x}_1}{h} \quad \boldsymbol{x}_2^* = \frac{\boldsymbol{x}_2}{h} \end{gathered} \tag{15}$$

3. RESULTS

Results intend to estimate the topology of the yield surfaces as well as the distribution of the adimensional variables λ, θ^*_{eq} and G^*_{eq} throughout the channel. In this paper the only input parameter that changes from one case to the other is the flow intensity, represented by the variable U^*, that is the average of u^* at the inlet. The rheological parameters are $G^*_0 = 1.0 \times 10^1$, $m = 1.0 \times 10^1$, $K = 1.0 \times 10^{-1}$, $n = 5.0 \times 10^{-1}$, $\eta^*_0 = 1.0 \times 10^4$ and $\eta^*_\infty = 1.0 \times 10^{-2}$. The problem statement is represented in Fig. 1, where $H = 4h$ and $l = L = 38.4h$. The computational domain is partitioning into a bi-linear Lagrangian finite element mesh for all primal variables with 4125 elements.

First, what all cases have in common will be discussed. The horizontal profile throughout the symmetric axis, $x^*_2 = 0$, of the variables θ^*_{eq}, λ and G^*_{eq} is shown in Fig. 3. At $x^*_2 = 0$ in the inlet the material is unyielded, the fluid is fully structured, $\lambda = 1$, $G^*_{eq} = G^*_0$ and $\theta^*_{eq} = \eta^*_0/G^*_0$. The flow of unyielded regions is called plug flow. Following the symmetric axis, the structuring level starts to decrease near the contraction where the unyielded zones vanish. Furthermore, G^*_{eq} reaches enormous values, that means an inelastic fluid. The topology of the yielded and unyielded zones are show in Fig. 2. After the contraction, the horizontal profiles recover the similar state of the inlet as the profile develops again. Watching the vertical profiles of λ, G^*_{eq} and θ_{eq} of Fig. 4, it is clear that in the yielded zones the material is stiff, as G^*_{eq} reaches great values near the wall. This increase on the G^*_{eq} leads θ^*_{eq} to zero in the yielded zones.

Comparing the unyielded regions for all cases from Fig. 2, when U^* increases the yielded height decreases and the material yields farther from the contraction. The location of the yield surfaces marks the change of λ, G^*_{eq} and θ^*_{eq}. The unyielded region in the corner of the contraction is bigger when the flow intensity is smaller, see Fig. 2.

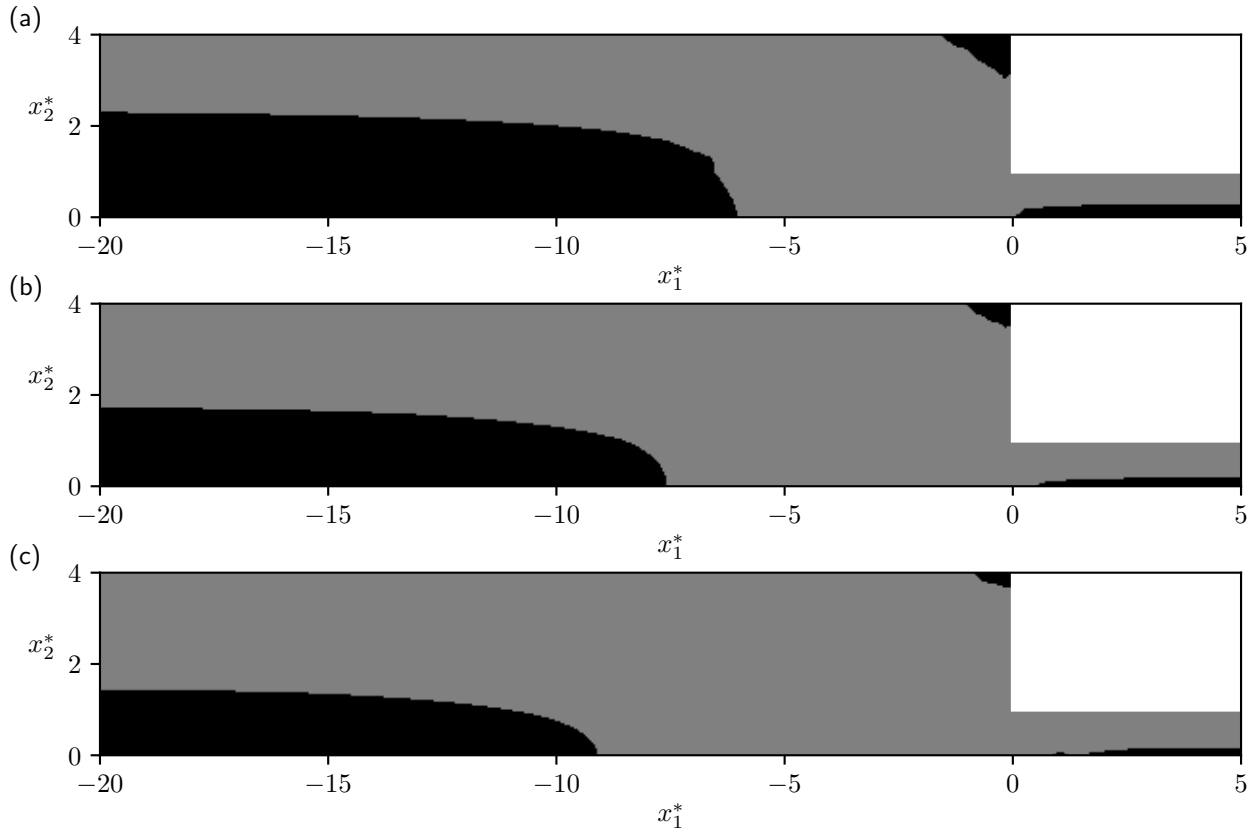

Figure 2: The effect of flow intensity on the yielded zones. The x^*_1 axis is shared along the charts (a) $U^* = 0.25$, (b) $U^* = 1.0$ and (c) $U^* = 2.0$. The zones in black the stress doesn't exceeds the yield stress, unyielded, and the yielded zones are in gray.

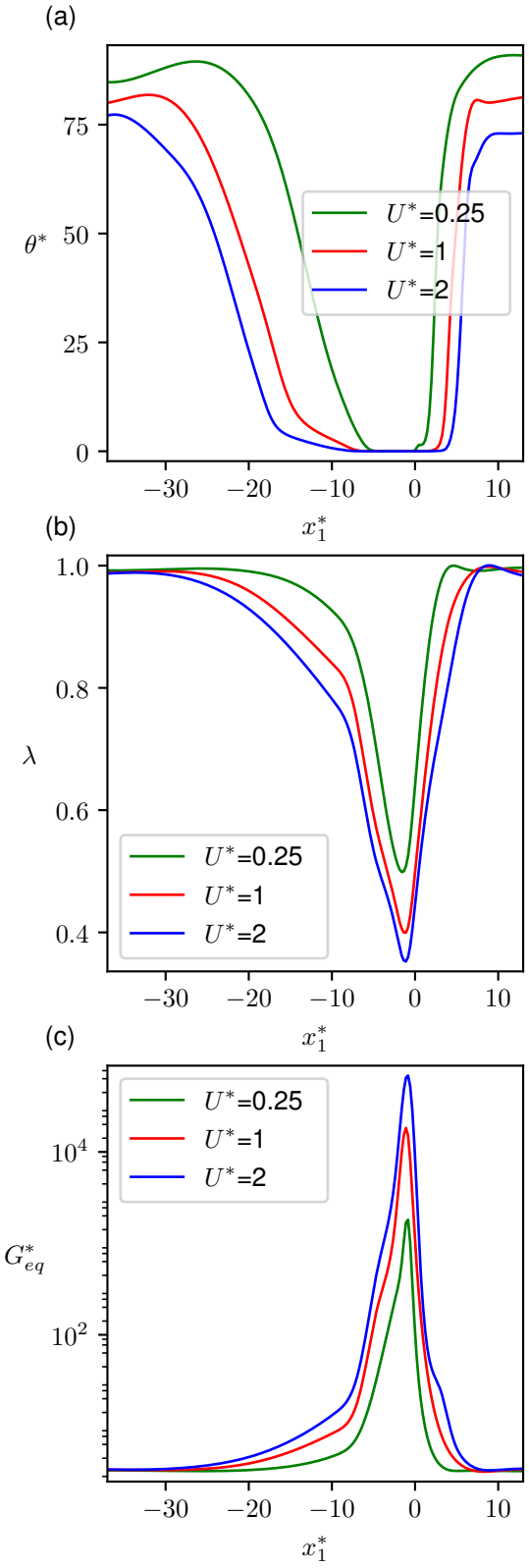

Figure 3: The influence of the flow intensity, $U^* = 0.25$, 1 and 2, at the symmetric axis, $x_2^* = 0$, on (a) adimensionalized equilibrium relaxation time, θ_{eq}^*, (b) structuring level λ and (c) adimensionalized elastic modulus G_{eq}^*.

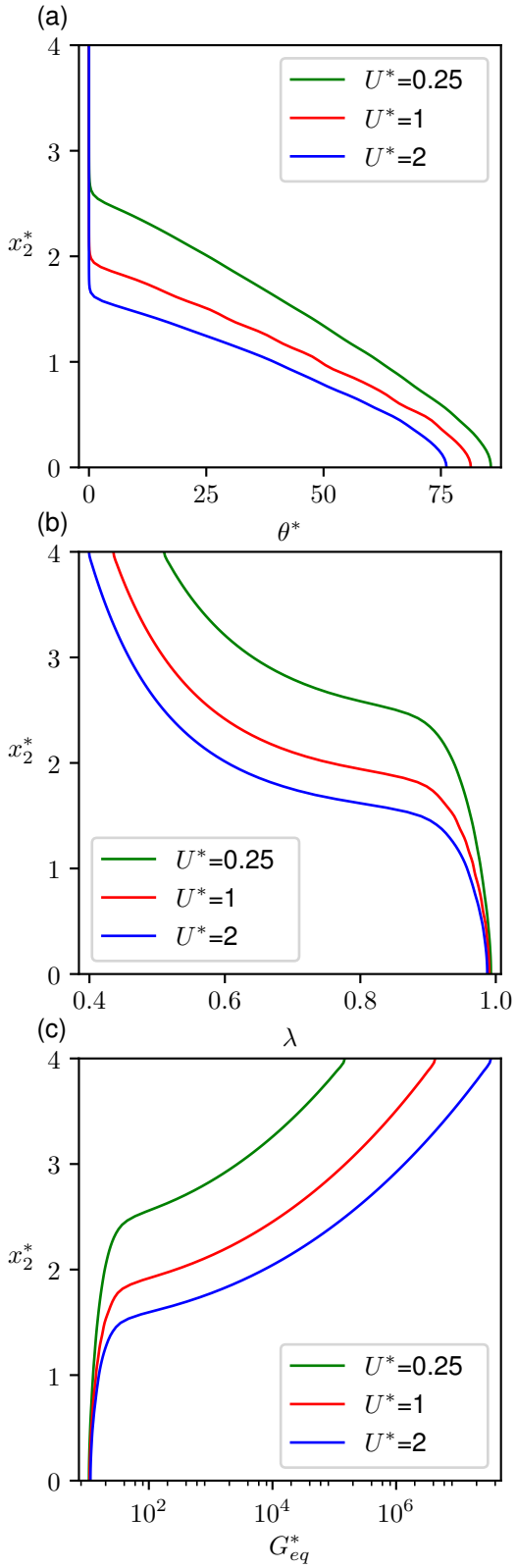

Figure 4: The influence of the flow intensity, $U^* = 0.25$, 1 and 2, at the inlet on (a) adimensionalized equilibrium relaxation time, θ_{eq}^*, (b) structuring level λ and (c) adimensionalized elastic modulus G_{eq}^*.

4. CONCLUSIONS

The flow of an elasto-visco plastic fluid is observed through a 4:1 axissymmetric contraction. It was verified that the flow intensity has a significant influence in the flow near the contraction. The increase of U^* shrinks the unyielded regions, where the yield surface marks the change on G^*_{eq} and θ^*_{eq}. For further studies, the goal is to analyze the influence of the contraction ratio and the loss of charge for elasto-visco plastic fluid flows.

5. ACKNOWLEDGMENTS

The author V. D. B. Abella thanks all the other authors N. A. Oliveira, S. Frey, M. F. Naccache and P. R. de Souza Mendes as well as the financial support by CNPq and CAPES.

6. RESPONSIBILITY NOTICE

The author is the only responsible for the printed material included in this paper.

7. REFERENCES

Balmforth, N.J., Frigaard, I.A. and Ovarlez, G., 2014. "Yielding to stress: Recent developments in viscoplastic fluid mechanics". *Annual Review of Fluid Mechanics*, Vol. 46, No. 1, pp. 121–146.

Barnes, H.A., 1999a. "A brief history of the yield stress". *Appl. Rheol*, Vol. 9, No. 6, pp. 262–266.

Barnes, H.A., 1999b. "The yield stress - a review or $\pi\alpha\nu\tau\alpha$ $\rho\varepsilon\iota$ - everything flows?" *Journal of Non-Newtonian Fluid Mechanics*, Vol. 81, No. 1-2, pp. 133–178.

Belblidia, F., Tamaddon-Jahromi, H.R., Webster, M.F. and Walters, K., 2011. "Computations with viscoplastic and viscoelastoplastic fluids". *Rheologica Acta*, Vol. 50, No. 4, pp. 343–360.

Bingham, E.C., 1922. *Fluidity and plasticity*, Vol. 2. McGraw-Hill.

Coussot, P., 2014. "Yield stress fluid flows: A review of experimental data". *Journal of Non-Newtonian Fluid Mechanics*, Vol. 211, pp. 31–49.

de Souza Mendes, P.R., 2007. "Dimensionless non-Newtonian fluid mechanics". *Journal of Non-Newtonian Fluid Mechanics*, Vol. 147, No. 1-2, pp. 109–116.

de Souza Mendes, P.R., 2011. "Thixotropic elasto-viscoplastic model for structured fluids". *Soft Matter*, Vol. 7, pp. 2471–2483.

de Souza Mendes, P.R. and Thompson, R.L., 2013. "A unified approach to model elasto-viscoplastic thixotropic yield-stress materials and apparent yield-stress fluids". *Rheologica Acta*, Vol. 52, No. 7, pp. 673–694.

de Souza Mendes, P.R.S. and Dutra, E.S.S., 2004. "Viscosity Function for Yield-Stress Liquids OVERVIEW OF THE AVAILABLE VISCOSITY". Vol. 14, No. 6, pp. 296–302.

Fraggedakis, D., Dimakopoulos, Y. and Tsamopoulos, J., 2016. "Yielding the yield stress analysis: A thorough comparison of recently proposed elasto-visco-plastic (EVP) fluid models". *Journal of Non-Newtonian Fluid Mechanics*, Vol. 236, pp. 104–122.

Franca, L.P. and Frey, S.L., 1992. "Stabilized finite element methods: II. The incompressible Navier-Stokes equations". *Computer Methods in Applied Mechanics and Engineering*, Vol. 99, No. 2-3, pp. 209–233.

Gueslin, B., Talini, L., Herzhaft, B., Peysson, Y. and Allain, C., 2006. "Flow induced by a sphere settling in an aging yield-stress fluid". *Physics of Fluids*, Vol. 18, No. 10.

Link, F.B., Frey, S., Thompson, R.L., Naccache, M.F. and de Souza Mendes, P.R., 2015. "Plane flow of thixotropic elasto-viscoplastic materials through a 1:4 sudden expansion". *Journal of Non-Newtonian Fluid Mechanics*, Vol. 220, pp. 162–174.

López-Aguilar, J.E., Webster, M.F., Tamaddon-Jahromi, H.R. and Manero, O., 2014. "A new constitutive model for worm-like micellar systems - Numerical simulation of confined contraction-expansion flows". *Journal of Non-Newtonian Fluid Mechanics*, Vol. 204, pp. 7–21.

López-Aguilar, J.E., Webster, M.F., Tamaddon-Jahromi, H.R. and Manero, O., 2016. "A comparative numerical study of time-dependent structured fluids in complex flows". *Rheologica Acta*, Vol. 55, No. 3, pp. 197–214.

Mahmood, R., Kousar, d.n., Yaqub, M. and Jabeen, K., 2017. "Numerical simulations of the square lid driven cavity flow of bingham fluids using nonconforming finite elements coupled with a direct solver". *Advances in Mathematical Physics*, Vol. 2017, pp. 1–10.

Nassar, B., de Souza Mendes, P.R. and Naccache, M.F., 2011. "Flow of elasto-viscoplastic liquids through an axisymmetric expansion-contraction". *Journal of Non-Newtonian Fluid Mechanics*, Vol. 166, No. 7-8, pp. 386–394.

Oishi, C.M., Martins, F.P. and Thompson, R.L., 2017. "The "avalanche effect" of an elasto-viscoplastic thixotropic material on an inclined plane". *Journal of Non-Newtonian Fluid Mechanics*, Vol. 247, pp. 165–177.

Park, Y.S. and Liu, P.L.F., 2010. "Oscillatory pipe flows of a yield-stress fluid". *Journal of Fluid Mechanics*, Vol. 658,

pp. 211–228.

Putz, A.M., Burghelea, T.I., Frigaard, I.A. and Martinez, D.M., 2008. "Settling of an isolated spherical particle in a yield stress shear thinning fluid". *Physics of Fluids*, Vol. 20, No. 3, pp. 1–12.

Rajagopalan, D., Armstrong, R.C. and Brown, R.A., 1990. "Finite element methdos for calculation of steady, viscoelastic flow using constitutive equations with a newtonian viscosity". *Journal of Non-Newtonian Fluid Mechanics*, Vol. 36, pp. 159 – 192.

Santos, D., Frey, S., Naccache, M. and De Souza Mendes, P., 2014. "Flow of elasto-viscoplastic liquids through a planar expansion-contraction". *Rheologica Acta*, Vol. 53.

Saramito, P., 2007. "A new constitutive equation for elastoviscoplastic fluid flows". *Journal of Non-Newtonian Fluid Mechanics*, Vol. 145, No. 1, pp. 1–14.

Saramito, P., 2009. "A new elastoviscoplastic model based on the Herschel-Bulkley viscoplastic model". *Journal of Non-Newtonian Fluid Mechanics*, Vol. 158, No. 1-3, pp. 154–161.

Sikorski, D., Tabuteau, H. and de Bruyn, J.R., 2009. "Motion and shape of bubbles rising through a yield-stress fluid". *Journal of Non-Newtonian Fluid Mechanics*, Vol. 159, No. 1-3, pp. 10–16.